ASPECTS OF POSTCLOSURE SAFETY OF THE MARK II ENGINEERED BARRIER SYSTEM FOR A USED FUEL REPOSITORY

E.P. Kremer
Nuclear Waste Management Organization, Toronto, Canada
ekremer@nwmo.ca

Abstract

The Nuclear Waste Management Organization is responsible for the implementation of Adaptive Phased Management, the federally-approved plan for the safe long-term management of Canada's used nuclear fuel. Under this plan, used nuclear fuel will ultimately be placed within a deep geological repository in a suitable host rock formation.

Before specific sites have been identified for detailed examination, generic studies are used to illustrate the long-term performance and safety of the multi-barrier repository system within various geological settings. The 6th and 7th Case Studies consider the postclosure safety of a repository that uses the Mark II engineered barrier system (EBS).

To be effective, the safety assessment must be robust and have an appropriate balance of model simplicity without excess conservatism. This paper considers how to approach a postclosure safety assessment of the Mark II EBS, with focus on the container failure model. Models representing the Normal Evolution Scenario are presented, including calculations and results.

1. Introduction

The full postclosure assessment methodology is based on guidance from the Canadian Nuclear Safety Commission [1]. The present paper considers in particular the Normal Evolution Scenario, which represents a likely or expected scenario. The assessment considers a one million year timeframe to cover key processes, including future glaciation, the potential for container failure, and maximum impact; if required, the timeframe will be extended to include maximum impact.

The repository's engineered barrier system (EBS) comprises the used fuel container and engineered sealing materials. The EBS is a key component of the design of the underground repository. The Mark II EBS consists of a carbon-steel, copper-coated used fuel container that is encapsulated within a bentonite buffer box.

One of the primary objectives of the 6th and 7th Case Studies is to illustrate the postclosure safety of a repository that uses the Mark II EBS. The used fuel container is a key component of the Mark II EBS and therefore the value of the safety assessment will depend greatly on how performance of the container is assessed.

2. Conceptual model for postulated container failure

Used fuel containers are designed to be long-lived and robust. The steel inner shell provides strength to resist the local pressure underground, the bentonite swelling pressure, and the pressure from future glaciations. The copper coating provides corrosion protection of the inner shell.

Containers will be manufactured according to a process that includes careful design, fabrication, closure welding, and a series of inspections to avoid significant defects. For the purpose of assessing repository performance, the postclosure safety assessment of the Mark II EBS will assume that a failure in the copper coating and inspection process could lead to containers placed in the repository with small defects in the copper coating.

This assumption is consistent with the preceding 4th and 5th Case Studies [2] [3], which consider an earlier container design, the IV-25. The 4th and 5th Case Studies assume that one out of 5,000 containers placed in the repository has an undetected defect in the copper shell weld. This rate is based on a review of failure statistics for other nuclear components [4] and is considered to be conservative for safety assessment purposes. The 4th and 5th Case Studies further assume the weld defect is 2 mm in diameter and spans the full 25 mm thickness of the copper (see Figure 1). Effectively, these assumptions require both that a substantive defect exists and that it is not detected by three separate inspections using different methods. Since the copper shell of the IV-25 container is not bonded to the steel and the steel lid is not welded to the steel vessel, the assessments assume groundwater can travel through the weld defect and then reach the fuel.

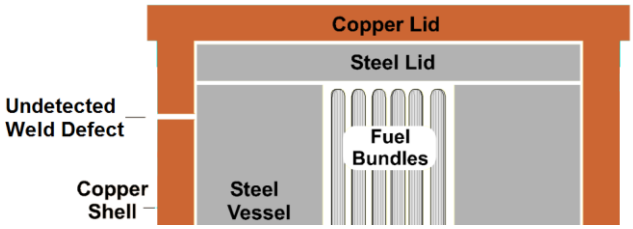

Figure 1 Conceptual illustration of the weld defect considered in 4th and 5th Case Studies.

The Mark II EBS includes numerous substantial improvements in the container design (see Figure 2): for example,

- The fine-grained copper coating permits detection of smaller defects.
- The copper barrier is bonded to the steel body, such that a through-copper defect will only expose steel immediately beneath the defect.
- In the event of a through-copper defect, the welded steel container will continue to act as a barrier to groundwater until corrosion of the steel perforates the container wall.

An important objective of the 6th and 7th Case Studies is to assess the postclosure safety of the Mark II EBS in a manner that credits these improvements in container design.

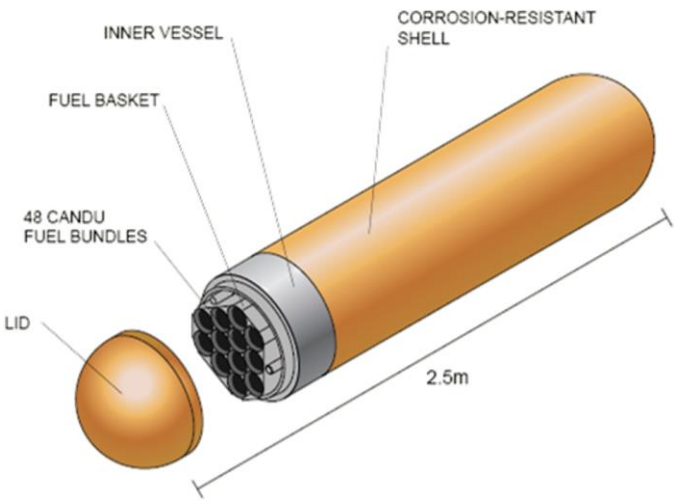

Figure 2 An illustration of the Mark II used fuel container.

3. Corrosion of the Mark II copper coating

As the repository environment becomes anoxic and dominated by reducing conditions, corrosion of the copper layer protecting the containers will occur primarily by reaction with groundwater sulphide and be limited by the rate of transport of sulphide through the buffer to the container surface.

Detailed characterization of specific sites will include comprehensive assessments of the deep groundwater, including dissolved sulphide concentrations. To date, assessments of the deep groundwaters in the Canadian Shield provide some information on sulphide concentrations. AECL reported dissolved sulphide to be "largely absent" [5]. Based on data in AECL field records (unpublished), any measurable groundwater sulphide is typically less than 1 µM; a single-point maximum was measured at 2.7 µM. There is typically no sulphide found in the groundwater in sedimentary rock [6].

In contrast, candidate geospheres for hosting repositories in other countries may present higher concentrations of groundwater sulphide: this paper considers Finland and Sweden.

3.1 Sulphide in the deep groundwater at Olkiluoto

In support of site characterisation, Posiva drilled deep boreholes to measure properties of their geosphere [7]. In several cases, open boreholes experienced considerable water flow, resulting in disturbed hydrogeochemical conditions. These disturbed conditions were associated with rapid biogeochemical dynamics and elevated concentrations of dissolved sulphides.

Elevated groundwater sulphide concentrations appear to equilibrate with amorphous iron sulphide (FeS); however, amorphous iron sulphide is unstable and rapidly converts to mackinawite within minutes to weeks, depending on conditions [7]. Also, disturbed conditions were observed to recover rapidly and appear to return to steady-state within years

to tens of years. Under stable hydrogeochemical conditions, the sulphide concentration in groundwater is instead controlled by pyrite (FeS_2).

PHREEQC reactive transport simulations [8] determined that, for a groundwater system controlled by amorphous iron sulphide, the dissolved sulphide concentration will settle between 1-10 µM. The same simulations determined that a groundwater system controlled by pyrite will present very low sulphide concentrations: as groundwater sulphide approaches equilibrium with pyrite, concentrations reduce to the detection limit (~0.3-0.6 µM); simulation results found equilibrium concentrations to settle between 10-40 pM (0.00001-0.00004 µM).

The Safety Case published by Posiva for their proposed repository at Olkiluoto [9] assumes what they describe as a "pessimistic upper bound" of 91 µM (3 ppm) groundwater sulphide, based on the possibility of solubility control by amorphous iron sulphide and the uncertainty of microbial activity.

3.2 Sulphide in the deep groundwater at Forsmark

SKB groundwater measurements of dissolved sulphide [10] found large inter-sample differences, leading to a conclusion similar to that reported by Posiva above – borehole drilling and sampling activities altered the original conditions and caused localised perturbations to the hydrochemical system, including transient peaks in sulphide concentrations. The report adds that, as groundwater measurements continue, these transient peaks are seen to decrease.

Figure 3 presents the cumulative distribution curve for groundwater sulphide concentrations used in the SR-Site assessment: sulphide concentrations have a 90th percentile value of 10 µM and a 50th percentile value of less than 1 µM.

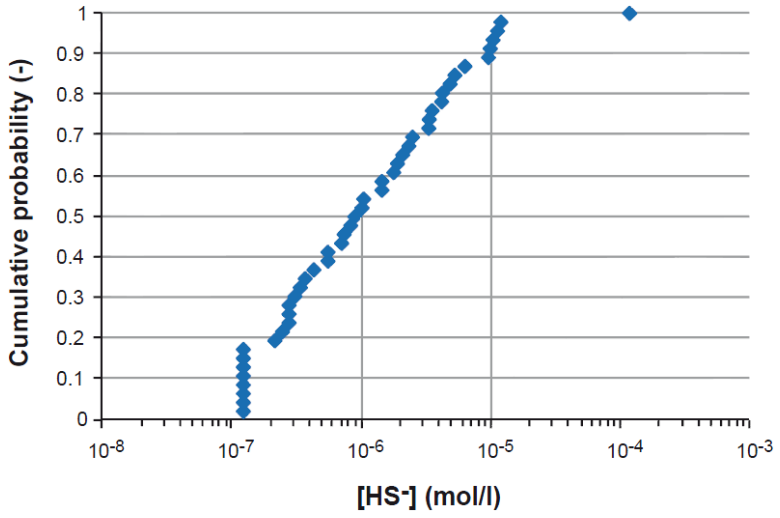

Figure 3 Sulphide concentrations in groundwaters at Forsmark [11]; data below detection are set to the lowest value measured, 0.12 µM.

After reviewing SKB's groundwater sampling and characterisation efforts, the Swedish regulator observed that "Sulphate reduction and production of sulphide is actively occurring in groundwaters at repository depth" [12].

For corrosion calculations for an intact buffer, the safety assessment completed by SKB for their proposed repository at Forsmark assumes the 90th percentile of measured groundwater sulphide concentrations, 10 µM [11].

3.3 Sulphide-limited copper corrosion rates

Information to date suggests groundwater within the host rock for the Canadian repository will contain almost no sulphide – likely below detection limits, substantially less than reported by either Posiva or SKB. It would be unrealistic and overly conservative for an assessment of the Mark II EBS to assume groundwater sulphide concentrations as high as either Posiva or SKB have used for their safety assessments. Calculations presented here assume the groundwater sulphide concentration is 1 µM, the 50th percentile of values reported by SKB for groundwaters at Forsmark and significantly higher than concentrations typically found in groundwaters in the Canadian Shield.

Corrosion rates presented here assume the copper layer protecting the containers will corrode primarily by reaction with groundwater sulphide; also, that the rate of corrosion will be limited by the amount of sulphide available [13]. Models developed by Briggs et al. [14] were used to calculate the rates of transport of sulphide from the host rock through the Mark II EBS to the container surface. Rates of sulphide transport were then used to calculate the corrosion rates presented in Figure 4 and Table 1.

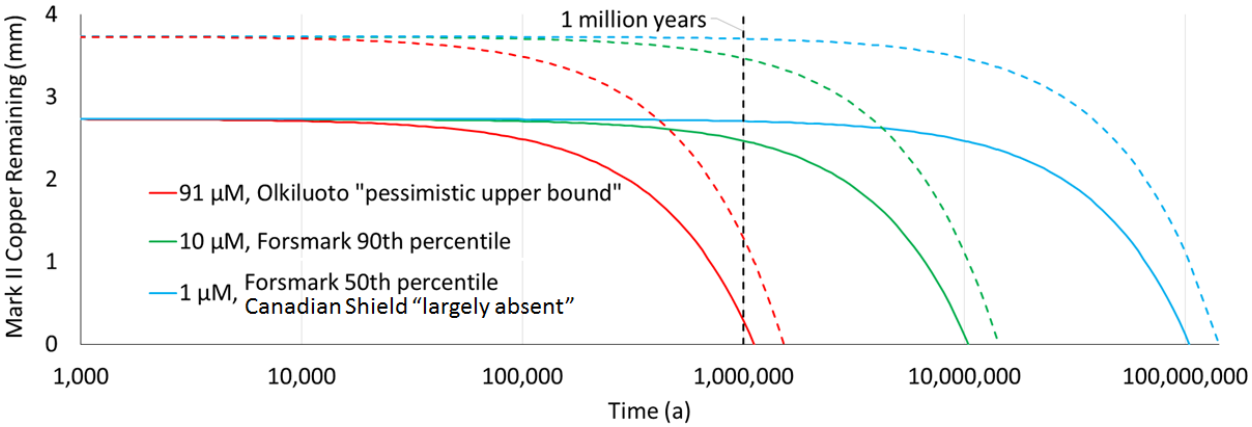

Figure 4 Reduction in the thickness of Mark II copper due to reaction with groundwater sulphide.

3.4 Defects in the copper coating

Design and characterization of the quality control (QC) technology that will confirm the thickness and continuity of the Mark II copper coating is ongoing. Work to date suggests

detection of coating defects that are 0.8 mm or larger is a realistic QC threshold. For a through-layer defect to pass QC inspection undetected is unlikely, perhaps unrealistic.

Table 1 Copper corrosion rates and associated loss of copper thickness.

	$[HS]_{GW}$ = 91 µM Olkiluoto "pessimistic upper bound"	$[HS]_{GW}$ = 10 µM Forsmark 90th percentile	$[HS]_{GW}$ = 1 µM Forsmark 50th percentile	$[HS]_{GW}$ = 1 µM Canadian Shield "largely absent"
Microbially-Influenced Corrosion (nm/a)	2.4	0.26	0.026	
Corrosion = 3 mm (Ma)	1.12	10.5	105	
Corrosion = 4 mm (Ma)	1.53	14.3	143	

The impact of an undetected defect on the local corrosion rate will depend partly on the size and shape of the defect. Figure 5 proposes some examples of hypothetical defects in a nominal 3 mm copper coating. If a defect results in locally thinner copper, steel beneath a defect may be exposed to groundwater earlier than calculations in Figure 4 suggest. Figure 6 and Table 2 present the time to exposed steel beneath a defect as a function of the defect size; calculations assume defects are oriented for maximum reduction in the local coating thickness; also, that corrosion of copper local to the defect is not slow relative to the uniform corrosion rate.

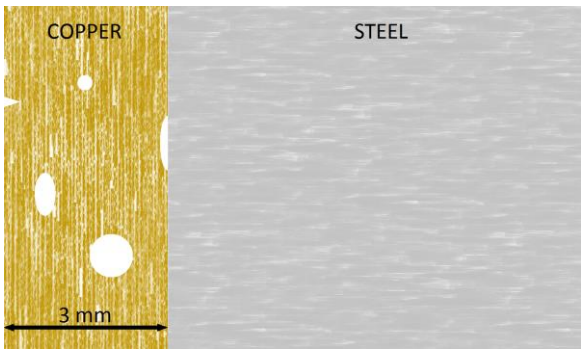

Figure 5 Hypothetical defects in the copper coating.

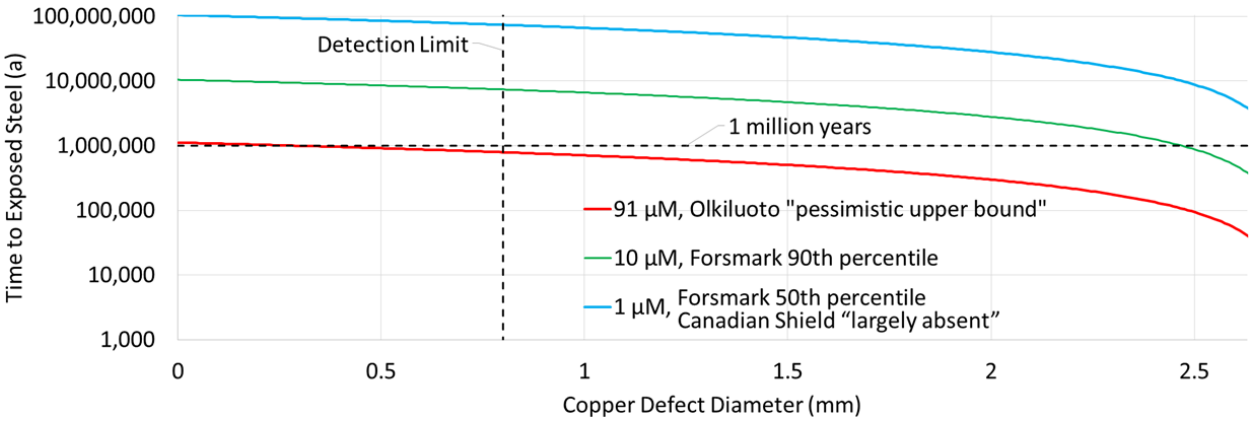

Figure 6 Time to exposed steel beneath defects in a nominal 3 mm copper coating.

For the purposes of assessing repository performance, the postclosure safety assessment of the Mark II EBS will consider a failure in the copper coating and inspection process that could lead to containers placed in the repository with small defects. Based on the results presented here, it may be reasonable and conservative to assume that defects passing QC inspection undetected would lead to exposed steel only after more than 10 million years. Defects leading to exposed steel within the one million year timeframe of the assessment would require a fairly large defect, greater than 2 mm, as well as elevated groundwater sulphide concentrations. Exposed steel upon placement in the repository would require a through-layer defect to pass QC inspection undetected, which may be unrealistic.

Table 2 Time to exposed steel beneath defects in a nominal 3 mm copper coating.

	$[HS]_{GW}$ = 91 µM *Olkiluoto* *"pessimistic upper bound"*	$[HS]_{GW}$ = 10 µM *Forsmark* *90th percentile*	$[HS]_{GW}$ = 1 µM *Forsmark* *Canadian Shield* *50th percentile* *"largely absent"*
Microbially-Influenced Corrosion (nm/a)	2.4	0.26	0.026
Corrosion = 3 mm (Ma)	1.12	10.5	105
Exposed Steel Time (Ma) Defect = 0.8 mm	0.79	7.4	74
Exposed Steel Time (Ma) Defect = 2 mm	0.30	2.8	28

4. Corrosion of the Mark II steel wall

If defects in the copper coating lead to exposed steel, groundwater will begin to corrode the exposed steel and may eventually perforate the wall of the container. The time required for groundwater to perforate a container will depend on the thickness of the steel wall (Figure 7) and on the steel corrosion rate.

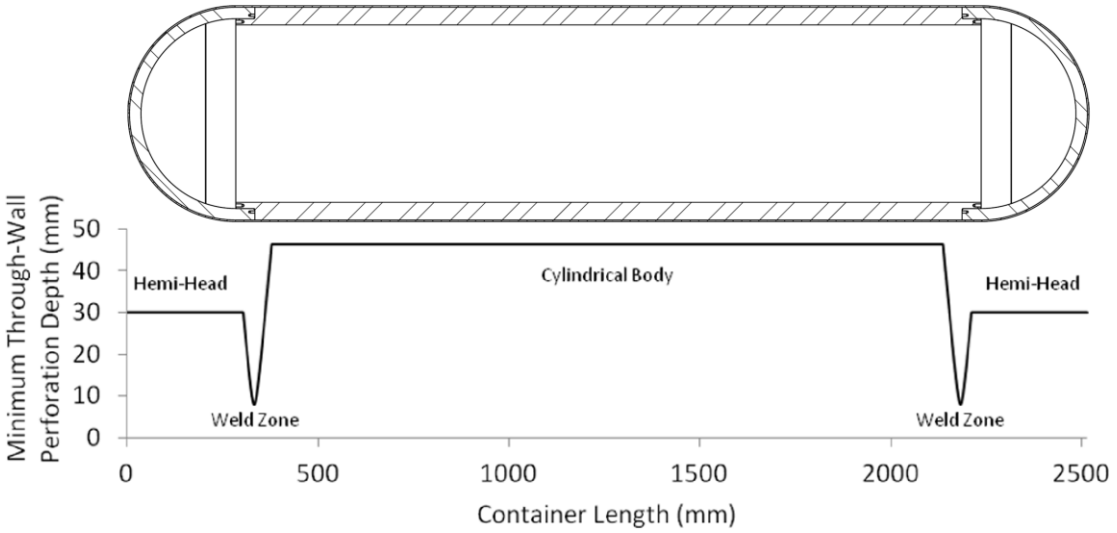

Figure 7 Minimum corrosion depth for through-wall perforation of Mark II steel container.

4.1 Steel wall thickness

The Mark II EBS container is protected by a continuous layer of copper. Although the container manufacturing and inspection processes are under development, presently there is no basis to assume there are any locations across the container surface where an undetected defect is more or less likely to occur. The postclosure safety assessment will assume an undetected defect is equally likely to occur anywhere across the container surface.

Sections of the container wall have different thicknesses. From the information provided in Figure 7,

- 70% of the container surface requires 46.2 mm of corrosion to perforate the container.
- 25.4% of the surface requires at least 30 mm of corrosion to perforate the container.
- 4.6% of the container surface requires something less than 30 mm of corrosion to perforate the container; the partial-penetration weld presents the minimum wall thickness of at least 8 mm and accounts for less than 1% of the container surface.

4.2 Rate of steel corrosion through a defect in the copper coating

The steel corrosion models used by the NWMO were developed by King [15]. Corrosion rates are temperature-dependent. The calculations discussed here use the container surface temperatures determined by Guo [16], shown in Figure 8. (This is a representative case, in the final design some containers may approach 100°C peak temperature.)

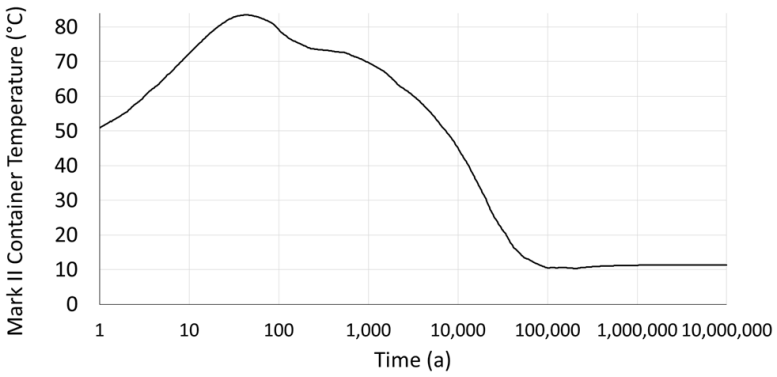

Figure 8 Evolution of Mark II EBS container surface temperature.

The postclosure repository environment will become anoxic within a relatively short time. Under these conditions, magnetite is the likely corrosion product, particularly if the system is carbonate-limited or only partially saturated; the rate of magnetite-generating corrosion is based primarily on work by Newman et al. [17]; passivation is implicit. Siderite may be the primary corrosion product if the system has sufficient carbonate available and is fully saturated; the rate of siderite-generating corrosion is based on literature values [15]; again, passivation is implicit. Rates for both forms of corrosion are shown in Figure 9, based on the

container temperatures provided in Figure 8. Siderite-generating corrosion is much faster than magnetite-generating corrosion – more than 10 times faster if temperatures are below ~40°C; in Figure 8, the temperature becomes less than 40°C around 14,000 years postclosure.

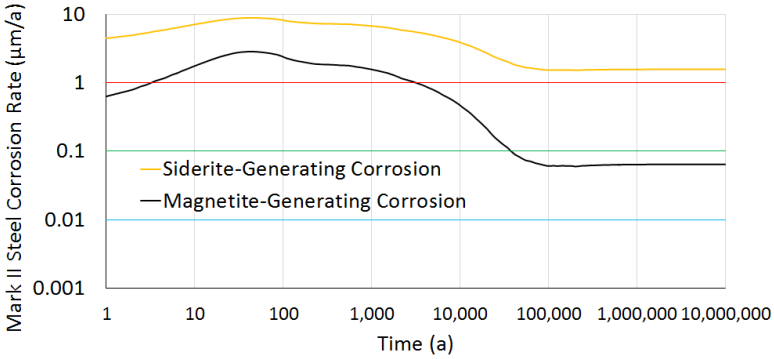

Figure 9 Evolution of steel corrosion rates.

The steel corrosion models developed by King [15] apply to an open surface with no protective copper coating, referred to here as open-surface corrosion. The models consider a corrosion front advancing uniformly through steel, where the corrosion product steadily suppresses the corrosion rate. These models may be adapted to reflect corrosion through a defect in the copper coating, referred to here as defect corrosion. Figure 10 illustrates how open-surface corrosion differs geometrically from defect corrosion: the corrosion front is expected to advance radially from the defect, resulting in an expanding hemisphere of corroded steel. This is supported by the micrograph included in Figure 10, presenting early results from laboratory experiments assessing defect corrosion of copper-coated steel.

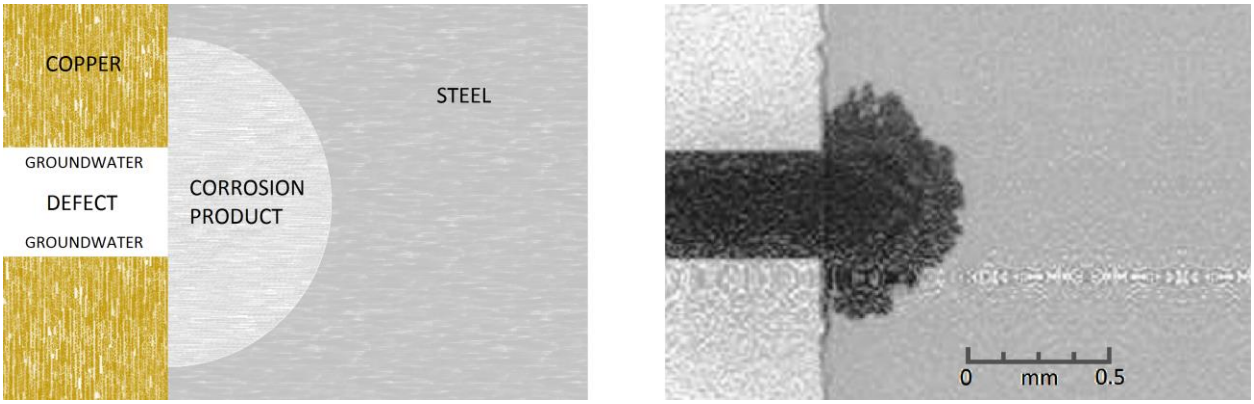

Figure 10 Conceptual illustration of defect corrosion (left panel); the micrograph (right panel) presents early results from laboratory experiments.

Assume the material properties of the corrosion product (bulk porosity, ion diffusivity, etc.) are the same under open-surface and defect corrosion. Considering the hemispherical corrosion front, it is then reasonable to infer that transport of the components of the corrosion reaction becomes dependent on the size of the defect. In this case, the rate of defect corrosion can be shown to relate to open-surface corrosion according to the following equation:

$$\frac{\text{Defect Corrosion}}{\text{Open–Surface Corrosion}} = \frac{r_0}{(r - r_0)}$$

where r_0 is the radius of the defect and r is the radius of steel lost to corrosion.

This relationship includes several potential conservatisms:

- For $r < r_0$, calculations assume open-surface corrosion.
- Corrosion products grown within the protected environment of the defect may be more homogenous and, consequently, more resistant to transport of reaction components.
- Expansion of corrosion product relative to corroded steel may further limit transport.
- Even if sufficient carbonate is available, this configuration may inhibit siderite-generating corrosion.

In addition, calculations presented here respect the lower bounds imposed on the open-surface corrosion models [15]. This addresses the uncertainty implicit in modelled defect corrosion rates not yet confirmed experimentally. Corrosion model calculations are shown in Figure 11 for both magnetite- and siderite-generating corrosion.

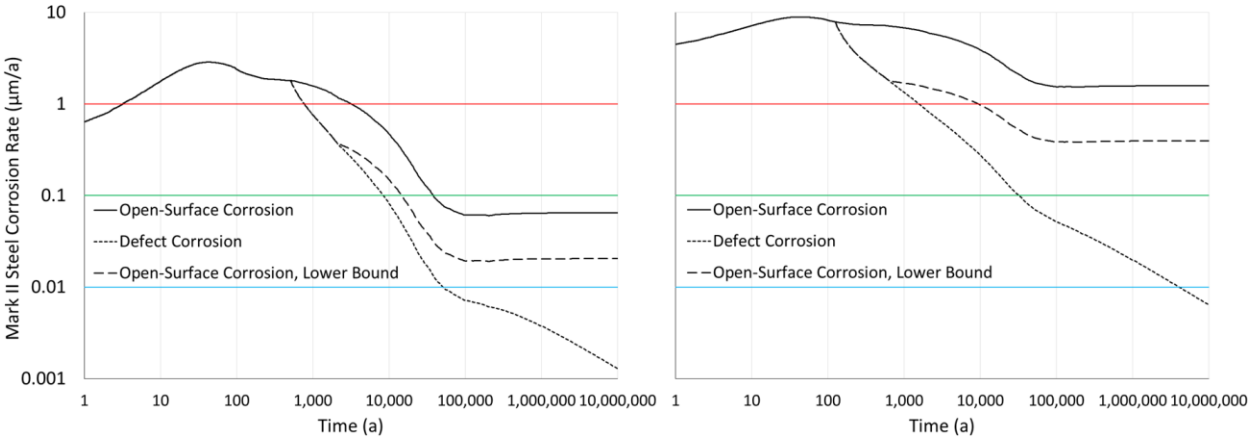

Figure 11 Adaption of open-surface corrosion models for defect corrosion, illustrated for magnetite-generating corrosion (left panel) and siderite-generating corrosion (right panel).

The corrosion model calculations shown in Figure 11 are used to determine the time required to perforate the different thicknesses of steel along the length of the container wall, shown in Figure 12. Table 3 provides a summary of perforation times. Depending on the modelled steel corrosion rate and the thickness of the steel wall, the time required for groundwater to perforate a container varies from as short as 1,100 years to well over 10 million years.

It should be noted that these calculations include corrosion rates driven by elevated temperatures associated with the first few thousands of years postclosure. As discussed above, for exposure of steel beneath a defect in the copper coating to occur within one million years

would require a fairly large defect, greater than 2 mm, as well as elevated groundwater sulphide concentrations. The steel corrosion calculations presented here assume exposed steel upon placement of containers in the repository. This would require a through-layer defect in the copper coating to pass QC inspection undetected, which may be unrealistic.

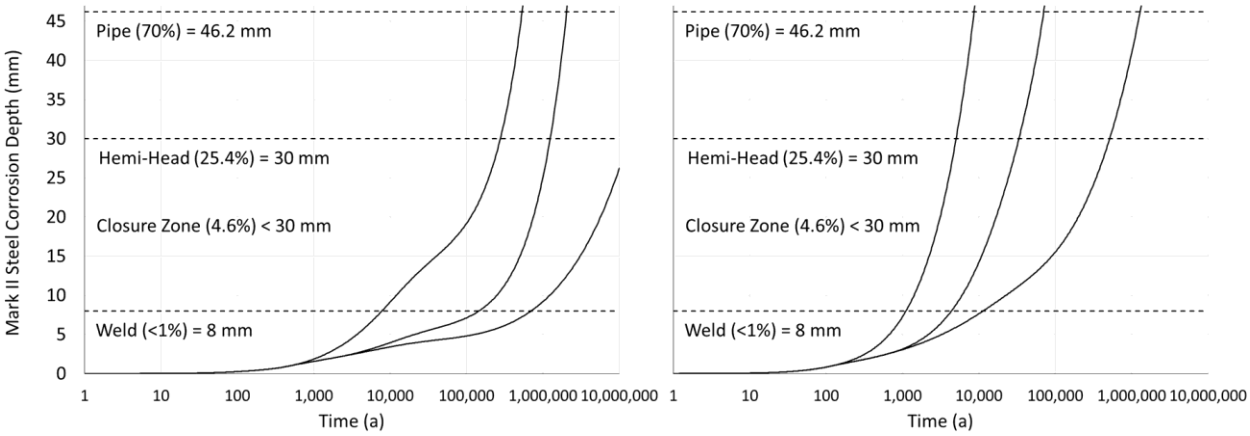

Figure 12 Evolution of steel corrosion depth using models illustrated in Figure 11.

Table 3: Time for steel corrosion to perforate the container wall.

	Cylinder Pipe (46.2 mm) *70% Container Surface* *Magnetite- / Siderite-Generating Corrosion*	*Hemi-Head (30 mm)* *25.4% Container Surface* *Magnetite- / Siderite-Generating Corrosion*	*Weld (8 mm)* *< 1% Container Surface* *Magnetite- / Siderite-Generating Corrosion*
Open-Surface Corrosion	530 ka / 8.6 ka	280 ka / 5 ka	7.8 ka / 1.1 ka
Defect Corrosion	>10 Ma / 1.3 Ma	>10 Ma / 510 ka	700 ka / 11 ka
Defect Corrosion with Lower Bound	2 Ma / 71 ka	1.3 Ma / 33 ka	140 ka / 4.4 ka

5. Conclusion

The postclosure safety assessment of the Mark II EBS will consider a failure in the copper coating and inspection process that could lead to containers placed in the repository with small defects. Corrosion modelling results presented here suggest it may be reasonable and conservative to assume that defects passing QC inspection undetected would lead to exposed steel only after more than 10 million years. Once steel is exposed to groundwater, corrosion model calculations find that the additional time required for groundwater to perforate a container may vary from as short as 1,100 years to well over 10 million years.

From these results, used fuel containers are expected to remain intact essentially indefinitely, with no releases (and no dose consequences) within the one million year timeframe of the postclosure safety assessment. This assumes all natural and engineered barriers function as intended, defined as the Reference Case of the Normal Evolution Scenario. However, in order to illustrate postclosure performance of the rest of the repository system, the Base Case of the

Normal Evolution Scenario will consider scenarios involving container failures. In this way, the 6th and 7th Case Studies can assess postclosure dose implications of the Mark II EBS.

6. References

[1] CNSC, "Regulatory Guide G-320: Assessing the Long Term Safety of Radioactive Waste Management", Canadian Nuclear Safety Commission, 2006.

[2] NWMO, "Used Fuel Repository Conceptual Design and Postclosure Safety Assessment in Crystalline Rock, Pre-Project Report", NWMO TR-2012-16.

[3] NWMO, "Postclosure Safety Assessment of a Used Fuel Repository in Sedimentary Rock, Pre-Project Report", NWMO TR-2013-07.

[4] Maak, P., P. Gierszewski and M. Saiedfar, "Early Failure Probability of Used-Fuel Containers in a Deep Geological Repository", OPG 06819-REP-01300-10022, 2001.

[5] Gascoyne, M. "The Evolution of Redox Conditions and Groundwater Chemistry in Recharge-Discharge Environments on the Canadian Shield", AECL-11682, 1996.

[6] INTERA, "OPG's Deep Geologic Repository for Low & Intermediate Level Waste, Descriptive Geosphere Site Model", NWMO DGR-TR-2011-24.

[7] Posiva, "Sulphide Fluxes and Concentrations in the Spent Nuclear Fuel Repository at Olkiluoto", Report 2014-01.

[8] Posiva, "Safety Case for the Disposal of Spent Nuclear Fuel at Olkiluoto – Models and Data for the Repository System 2012", Report 2013-01.

[9] Posiva, "Safety Case for the Disposal of Spent Nuclear Fuel at Olkiluoto – Performance Assessment 2012", Report 2012-04.

[10] SKB, "SR-Site – Sulphide Content in the Groundwater at Forsmark", TR-10-39, 2010.

[11] SKB, "Corrosion Calculations for the Safety Assessment SR-Site", TR-10-66, 2010.

[12] SSM, "Independent Assessment of Groundwater Sulphide Content in the Long-Term", Technical Note 2014:48, 2014.

[13] Scully, J.R. and M. Edwards. "Review of the NWMO Copper Corrosion Allowance", NWMO TR-2013-04.

[14] Briggs, S. J. McKelvie, P. Keech, B. Sleep and M. Krol, "Transient Modelling of Sulphide Diffusion under Thermal Conditions Typical of a DGR", Proceedings of the 6th International Workshop on Long-Term Corrosion, Toronto, Canada, 2016 May 9-12.

[15] King, F. "Consequences of the General Corrosion of Carbon Steel Used Fuel Containers for Gas Generation in a DGR", NWMO TR-2013-16.

[16] Guo, R. "Thermal Response of a Mark II Conceptual Deep Geological Repository in Crystalline Rock", NWMO TR-2016-03.

[17] Newman, R.C., S. Wang and G. Kwong, "Anaerobic Corrosion Studies of Carbon Steel Used Fuel Containers", NWMO TR-2010-07.